2018 IEEE International Conference on Robotics and Automation (ICRA)
May 21-25, 2018, Brisbane, Australia

Stability and Predictability in Dynamically Complex Physical Interactions

Salah Bazzi
Department of Biology
Department of Electrical and Computer Engineering
Northeastern University
Boston, Massachusetts 02115
s.bazzi@northeastern.edu

Julia Ebert
School of Engineering and Applied Sciences
Harvard University
Cambridge, Massachusetts 02138
ebert@g.harvard.edu

Neville Hogan
Department of Mechanical Engineering
Department of Brain and Cognitive Sciences
Massachusetts Institute of Technology
Cambridge, Massachusetts 02139
neville@mit.edu

Dagmar Sternad
Department of Biology
Department of Electrical and Computer Engineering
Northeastern University
Boston, Massachusetts 02115
D.Sternad@northeastern.edu

Abstract— **This study examines human control of physical interaction with objects that exhibit complex (nonlinear, chaotic, underactuated) dynamics. We hypothesized that humans exploited stability properties of the human-object interaction. Using a simplified 2D model for carrying a "cup of coffee", we developed a virtual implementation to identify human control strategies. Transporting a cup of coffee was modeled as a cart with a suspended pendulum, where humans moved the cart on a horizontal line via a robotic manipulandum. The specific task was to transport the cart-pendulum system to a target, as fast as possible, while accommodating assistive and resistive perturbations. To assess trajectory stability, we applied contraction analysis. We showed that when the perturbation was assistive, humans absorbed the perturbation by controlling cart trajectories into a contraction region prior to the perturbation. When the perturbation was resistive, subjects passed through a contraction region following the perturbation. Entering a contraction region stabilizes performance and makes the dynamics more predictable. This human control strategy could inspire more robust control strategies for physical interaction in robots.**

I. Introduction

Compared to modern-day robots, human actuation is inferior in both bandwidth and speed of information transmission. Despite this fact, humans display superior agility and dexterity, especially when they are physically interacting with dynamically complex objects. This disparity in performance raises the question of how humans achieve their remarkable dexterity. Better understanding of human motor control might inform advances in the control of robots, exoskeletons and prostheses.

Insights gained in human motor control have helped inspire new ways to address problems in robot motion and control. For example, the framework of dynamic movement primitives for motor control in robotics is closely related to Central Pattern Generators (CPG) in neurobiology [1]. Building upon recent advances in the control of the human hand during grasping, Ciocarlie et al. [2] [3] devised a grasp planning algorithm that operates on a hand posture subspace of highly reduced dimensionality. Recently, Ott et al. [4] showed on a humanoid robot that a biologically inspired posture control approach is more robust than a model-based one. Inspired by human motor learning principles, Gehring et al. [5] devised a method for fine-tuning the parameters of a quadruped robot controller by introducing slight variations over repeated motions. Sugimoto et al. [6] were able to efficiently improve the movement policy of a humanoid robot using a limited number of samples from its real environment. Further, in physical human-robot interaction a recent study showed that interaction was facilitated when the robot movement closely resembled natural human movement [7]. These examples demonstrate that applying insights from biological motor control principles may prove useful for robot motor control and human-robot interaction.

This study examined the control strategies that humans employ when physically (and skillfully) interacting with dynamically complex objects. In particular, we studied the task of transporting a cup of coffee in the presence of visible and predictable external perturbations. The task was rendered in a virtual environment using a robotic manipulandum [8] and perturbations either resisted or assisted the motion. Such a task poses a challenge due to the underactuated, nonlinear, and chaotic dynamics of the object. Moreover, object interaction introduces bidirectional forces that pose a control challenge absent in free movements [9].

It is generally assumed that humans acquire an internal model of the task to predict object dynamics and thereby afford inverse dynamics control [10] [11] [12] [13]. However, control based on internal models for physical interaction with objects exhibiting nonlinear and underactuated dynamics appears challenging. Furthermore, relying on feedback cor-

This work is supported by the following grants awarded to Dagmar Sternad: NIH R01-HD087089, NSF-EAGER 1548514, NSF-NRI 1637854. N. Hogan was supported in part by the Eric P. and Evelyn E. Newman Fund, NSF-EAGER 1548501, NSF-NRI 1637824, NIH R01-HD087089.

rections is not plausible due to the relatively long feedback delays in the neuromotor system. We therefore hypothesized that rather than learning accurate and precise models, humans seek to make interactions predictable. Predictability implies that expected uncertainties in the future, and their effects, are minimized.

We operationalize predictability in terms of stability: A stable system rejects small perturbations and returns to its stable orbit, which is predictable. We hypothesized that humans learn such stable and predictable trajectories to obviate error corrections and extensive computations based on accurate and precise models of nonlinear dynamics. This strategy provides robustness in the face of external perturbations and model-based closed-loop control becomes less critical.

To measure stability and convergence of a given trajectory, we used contraction theory [14]. Contraction analysis assesses stability of nonlinear systems by studying convergence between trajectories. Contraction theory is well-suited to the problem at hand since we are not interested in the final nominal behavior, such as equilibrium points or limit cycles, but rather in those trajectories that forget initial conditions, noise, and perturbations. Regions of the state space in which neighboring trajectories converge to each other are contraction regions.

This study shows that humans indeed exploit contraction regions to deal with perturbations during dynamically complex physical interactions. In particular, we show that humans exploit the contraction regions of the free, unforced system. This is energetically efficient since the system is driven to a state where its natural, passive dynamics guide it to convergence and there is no need to exert any extra effort.

This paper is organized as follows. A review of some of the main results of contraction analysis is provided in Section II. Section III details the task, its simplified model, and the experimental paradigm. Section IV presents computations of the contraction regions. Section V tests the hypothesis and assesses the human trajectories with respect to the contraction regions. Section VI explores directions for future work.

II. Background

Lohmiller and Slotine [14] developed contraction analysis as a method for *differentially* analyzing stability and convergence of nonlinear systems, by quantifying the convergence of neighboring trajectories.

Consider the general form of a nonlinear system

$$\dot{x} = f(x,t), \tag{1}$$

where f is an $n\times 1$ nonlinear vector function and x is an $n\times 1$ state vector. This equation may also represent the closed-loop dynamics of a control system with a feedback controller $u(x,t)$.

Next, consider two neighboring trajectories, $x_1(t)$ and $x_2(t)$, representing two solutions of (1) for two different initial conditions x_1^0 and x_2^0 respectively. A virtual infinitesimal displacement between the trajectories at a fixed time is δx, as illustrated in Figure 1.

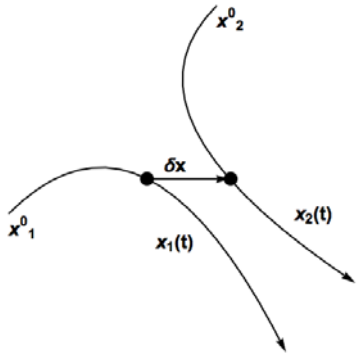

Fig. 1. Virtual displacement δx between two neighboring solutions $x_1(t)$ and $x_2(t)$ of $\dot{x} = f(x,t)$.

From (1), the differential is

$$\delta\dot{x} = \frac{\partial f}{\partial x}(x,t)\delta x. \tag{2}$$

Thus, the rate of change of the squared distance between these trajectories is

$$\frac{d}{dt}(\delta x^T \delta x) = 2\delta x^T \frac{\partial f}{\partial x}\delta x. \tag{3}$$

Any length $\|\delta x\|$ converges exponentially to zero if the Jacobian $\frac{\partial f}{\partial x}$ is uniformly negative definite. Any region of the state space in which the Jacobian satisfies this negative definite condition is referred to as a contraction region. For the Jacobian to be uniformly negative definite, this means that

$$\exists \beta > 0, \forall x, \forall t \geq 0, \frac{1}{2}(\frac{\partial f}{\partial x} + \frac{\partial f^T}{\partial x}) \leq -\beta \mathbf{I} < \mathbf{0}. \tag{4}$$

In this case, all the eigenvalues of the symmetric part of the Jacobian need to be uniformly negative definite. However, this is only a sufficient condition for exponential convergence.

A necessary and sufficient condition for exponential convergence can be formulated by a more general definition of differential length. Consider a differential coordinate transformation of the form

$$\delta z = \Theta(x,t)\delta x, \tag{5}$$

where $\Theta(x,t)$ is a square matrix that satisfies $\Theta^T\Theta > 0$. Θ is referred to as the contraction metric. In this new coordinate frame, a contraction region is one that satisfies

$$\frac{1}{2}(F + F^T) < 0, \tag{6}$$

where F is the generalized Jacobian

$$F = (\dot{\Theta} + \Theta\frac{\partial f}{\partial x})\Theta^{-1}. \tag{7}$$

All eigenvalues of the symmetric part of the generalized Jacobian F must be uniformly negative definite. Therefore, a necessary and sufficient condition for a region of the state

space to be contracting is that there exist a metric Θ such that $\Theta^T\Theta > 0$ and $\frac{1}{2}(F + F^T) < 0$ over that region. If this condition is satisfied, any trajectory starting in a ball of constant radius (with respect to the metric), centered on a given trajectory that is contained at all times in a contraction region with respect to that metric, remains in that ball and converges exponentially to that trajectory.

It is important to mention that finding a suitable metric is not trivial, and can be the most challenging part of contraction analysis. Several methods have been proposed for obtaining a metric, including semi-definite programming [15] and sums-of-squares programming [16]. This study will use a method based on solving a partial differential equation to arrive at a suitable metric.

III. The Cup-of-Coffee Task Experiment

Transporting a cup filled with coffee is an example of physical interaction with a dynamically complex object; moving the cup causes sloshing of the coffee, which in turn exerts forces on the cup and the hand, i.e., the task requires interacting with complex nonlinear fluid dynamics. In the experimental task subjects transported this underactuated object from a start point to an end point, while traversing a visible perturbation along the way. Magnitude and direction of the perturbation are known and subjects could learn the best strategy in 60 trials.

A. Mechanical Model of the Task

Simulating a realistic 3D cup with sloshing coffee with nonlinear equations from fluid mechanics is computationally expensive, especially when representing the system in a virtual environment. In addition, analytical treatment becomes vastly more challenging. Therefore, the task was simplified to a semicircular 2D arc with a ball rolling inside. The motion of the cup was limited to one direction along the horizontal axis. Assuming that the ball does not roll and only slides without friction along the cup, the system becomes mathematically equivalent to the well-known cart-pendulum system, with the pendulum being undamped. Despite this simplification, much of the complex dynamic behavior was retained. Figure 2 illustrates the real task (Fig. 2A), the conceptual model (Fig. 2B), and the mechanical model (Fig. 2C).

The equations of motion of the mechanical model are

$$(m+M)\ddot{x}(t) = lm\left(\dot{\phi}(t)^2\sin(\phi(t)) - \ddot{\phi}(t)\cos(\phi(t))\right) + u - b\dot{x}(t), \quad (8)$$

$$l\ddot{\phi}(t) = -g\sin(\phi(t)) - G\ddot{x}(t)\cos(\phi(t)), \quad (9)$$

where $x(t)$ denotes the position of the cart, $\phi(t)$ denotes the pendulum angle with a counterclockwise positive convention, m is the mass of the pendulum, M is the mass of the cart, l is the length of the massless pendulum rod, and g is the gravitational acceleration. The force exerted by the human subject is u. For contraction regions to exist, there must be some form of energy dissipation. Therefore damping was added in the x coordinate, with the damping coefficient

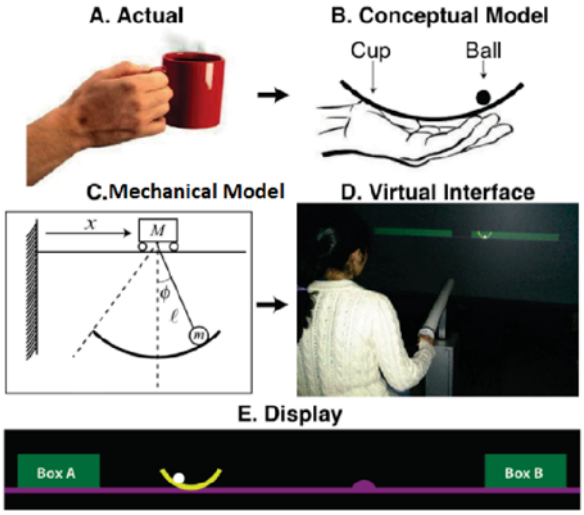

Fig. 2. Different models of the cup task (A, B, C) and the virtual interface (D, E).

denoted by b. Applied to the horizontal displacement of the cart, this damping may arise from human arm impedance. To increase the task challenge and to exclude the trivial case where the contraction region spans the entire state space, the cup acceleration $\ddot{x}$ was multiplied by a gain G. This makes the ball more responsive to movements of the cup when implemented in the virtual environment. The parameters used to simulate the cup task in the virtual environment were: $M = 3.5$kg, $m = 0.3$kg, $l = 0.35$m, $b = 20$N.s/m, and $G = 5$.

B. The Experimental Virtual Task

This simplified mechanical model was simulated in a virtual environment with visual and haptic feedback interfaced with a robotic manipulandum, as depicted in Fig. 2D. The projection screen displayed a cup (corresponding to the cart) and ball (corresponding to the pendulum bob), as seen in Fig. 2E. Participants were asked to move the cup from the start box A to the target box B as fast as possible. In addition, the cup should come to rest in box B without the ball rolling beyond the rim of the cup and escaping. At 60% of the travel distance, a perturbation of magnitude 40N and duration 20ms was applied to the cup in the horizontal direction. The forces either assisted or resisted the cup, *i.e.* acted either in the direction of motion of the cup or against it. The position of the perturbation was visually displayed as a bump on the horizontal line (Fig. 2E) and the subject always knew the magnitude and the direction of the perturbation as they were presented in blocks.

The experiment consisted of 4 blocks. To familiarize participants with the task, block 1 did not present any perturbation and subjects just moved from left to right. Blocks 2 and 4 comprised 60 trials each and involved assistive and resistive perturbations respectively. Block 3 comprised 10 baseline trials between the two perturbation blocks. At the beginning of each trial, the cup was centered in box A and the ball rested at its equilibrium position.

C. Apparatus and Data Acquisition

The participants in the experiment were seated in front of a large projection screen (2.4×2.4m) at about 2m distance. Physical interaction with the virtual environment was via a 3-degree-of-freedom force-controlled robotic manipulandum (HapticMaster, Motekforce, NL [8]). By applying a force to the handle of the robotic arm, participants controlled the horizontal x-position of the virtual cup. The robotic arm was restricted to move only in the horizontal direction along the subject's frontal plane to ensure a uni-directional motion of the cup, consistent with the model. The robotic arm provided haptic feedback, allowing participants to sense the system's inertia, the force of the ball on the cup, and the perturbations. More details on the manipulandum's end-effector position resolution, haptic resolution, and force sensitivity, are provided in [8].

The force applied by the participants to the manipulandum (u) and the kinematics of the cup and the ball ($x, \dot{x}, \ddot{x}, \phi, \dot{\phi}, \ddot{\phi}$) were all recorded at 120 Hz. Data was collected from four subjects.

IV. Analysis of Contraction Regions

To compute the contraction regions of the model (8) and (9), the equations were re-written in their state-space representation. Taking $X = (\dot{x}, \phi, \dot{\phi})^T = (x1, x2, x3)^T$, the state-space equations are

$$\dot{X} = \begin{pmatrix} \ddot{x} \\ \dot{\phi} \\ \ddot{\phi} \end{pmatrix} = \begin{pmatrix} \dot{x}1 \\ \dot{x}2 \\ \dot{x}3 \end{pmatrix} = \begin{pmatrix} \frac{-bx1+u+gm\sin(x2)\cos(x2)+lmx3^2\sin(x2}{-Gm\cos^2(x2)+m+M} \\ x3 \\ \frac{G\cos(x2)(u-bx1)+g(m+M)\sin(x2)+Glmx3^2\sin(x2)\cos(x2)}{Glm\cos^2(x2)-l(m+M)} \end{pmatrix}. \tag{10}$$

For a region to be contracting, the Jacobian must be uniformly negative definite in this region. For the parameterized model, the symmetric part of the Jacobian, J_{sym}, for the free uncontrolled system ($u = 0$) was not found to be negative definite for any point in the state space. However, this did not rule out the existence of contraction regions, since the condition on negativity of J_{sym} is only a sufficient one.

The next step was to find a contraction metric $\Theta(X, t)$ for which some regions of the state space would be contracting. The partial differential equation provided in [14] for computing a suitable metric revealed the contraction regions

$$\frac{\partial \Theta}{\partial X} f + \Theta J = -\Theta, \tag{11}$$

where f is the nonlinear vector function describing the dynamics (10) and J is the Jacobian $\frac{\partial f}{\partial X}$. This partial differential equation was solved numerically to obtain the contraction metric, which then enabled the computation of the generalized Jacobian F from (7). To deduce the contraction regions, the negativity condition (6) was tested for points in the state space within the range

$$-0.2 \leq \dot{x} \leq 0.7; \quad -1.5 \leq \phi \leq 1.5; \quad -6 \leq \dot{\phi} \leq 6.$$

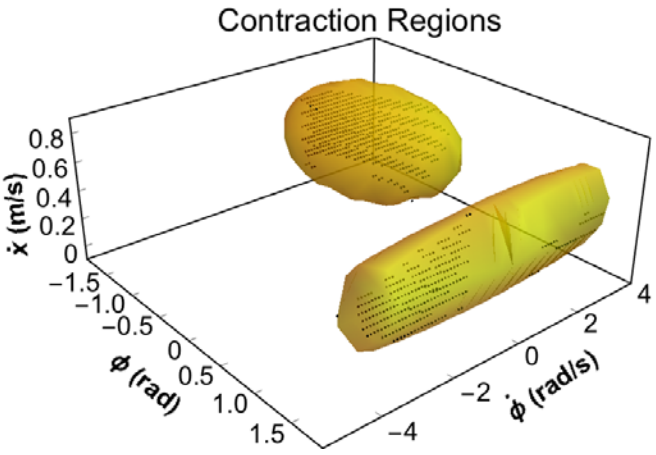

Fig. 3. Contraction regions in the state space of the cart-pendulum (cup-ball) system. The black points indicate states that satisfied the negativity condition (6). The yellow contraction regions are the minimum volume ellipsoids that contain these points.

These boundaries were used since human subject's data were confined to this range. The points in the state space that satisfied the condition were therefore elements of a contraction region. Figure 3 displays these contraction regions.

V. Experimental Results

As the contraction regions have been computed, the human data were evaluated with respect to the contraction regions. The goal was to test the hypothesis that humans take advantage of the contraction regions to absorb or exploit the perturbations.

A. Assisting Perturbations

Figure 4 illustrates one early trial and one late trial for one exemplary subject in the block with assisting perturbations. For ease of interpretation, the trajectories and the contraction regions have been projected onto the $\phi - \dot{\phi}$ plane. In the early trials, the trajectories did not pass through any contraction regions. However, after some practice, the contraction region was entered just prior to the perturbation. This caused the perturbation to occur within the contraction region, thereby mitigating instability and increasing predictability.

This strategy is effective as it reduces divergence and the probability of chaotic and unpredictable behavior. Figure 5 presents one late trial in the full 3 dimensions of the state space. The same changes of strategy were observed in four other subjects.

B. Resistive Perturbations

Figure 6 illustrates an early and a late trial for one subject when performing the task with a resistive perturbation. For ease of interpretation, the human trajectories and the contraction regions have been projected onto the $\phi - \dot{\phi}$ plane. As for assistive perturbations, early trials did not make use of the contraction regions. However, as the subject learned to navigate the perturbations, the strategy changed and the trajectory passed through a contraction region after the perturbation. This attenuated the transient effects of the

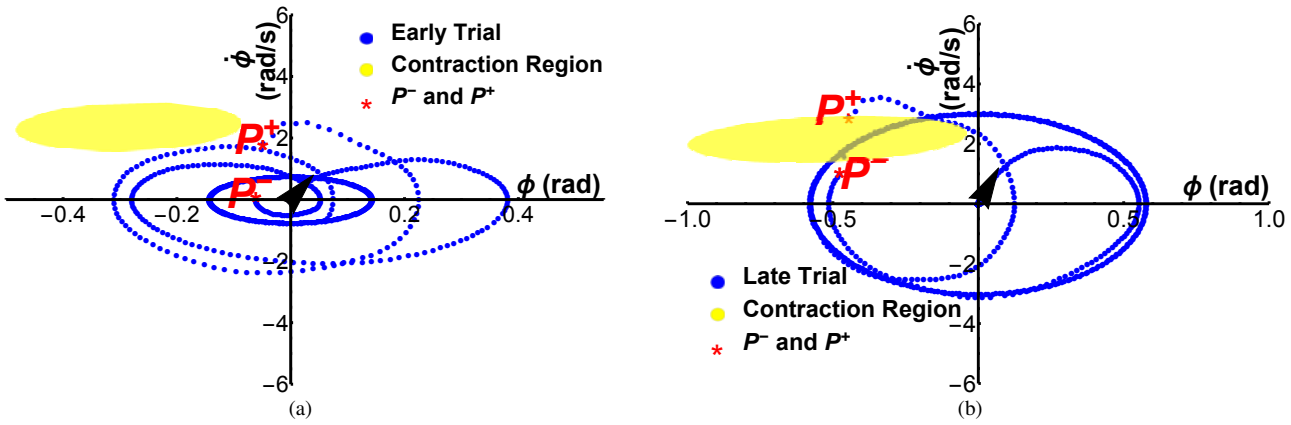

Fig. 4. Human trajectories for the condition with assisting perturbation: (a) Early trial (b) Late trial. P^- denotes the instant just before the perturbation while P^+ denotes the instant after the perturbation. The system starts at $(0, 0)$.

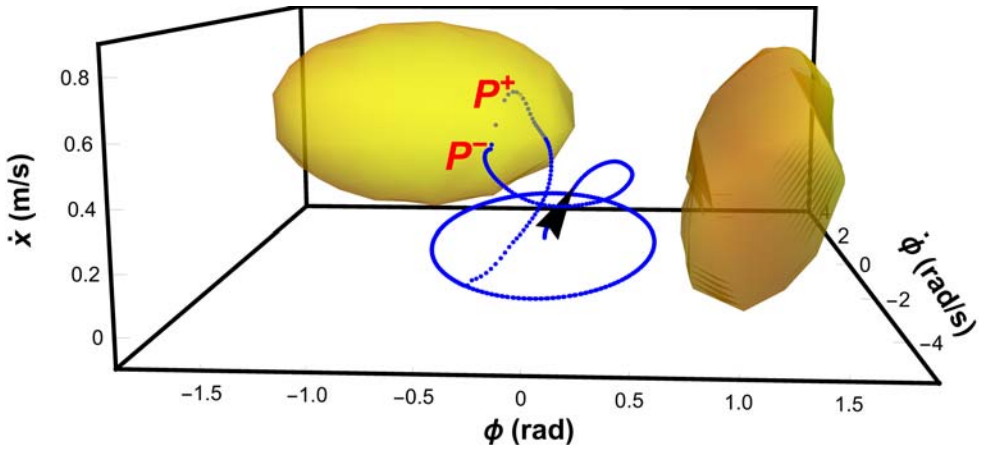

Fig. 5. One late trial with assisting perturbations. The subject learned the perturbation and shapes the trajectory to arrive at a contraction region.

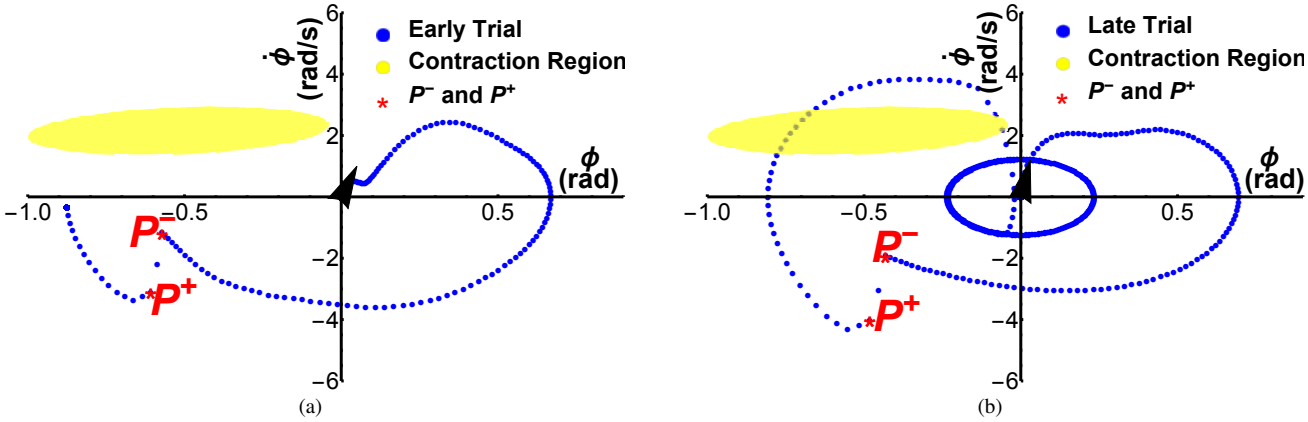

Fig. 6. Human trajectories for resistive perturbation: (a) Early trial (b) Late trial. P^- denotes the instant just before the perturbation while P^+ denotes the instant after the perturbation. The initial conditions are $(0, 0)$.

perturbation and stabilized the trajectory, thereby increasing predictability. The same pattern was observed in all four subjects. Figure 7 presents a different late trial in the full 3 dimensions of the state space.

The differences between the control strategies for assistive and resistive perturbations are noteworthy. For an assistive perturbation, the velocity of the cart increased and hence there was a greater risk of onset of chaotic and unpredictable dynamics. This is why subjects chose to absorb the perturbation immediately. In contrast, a resistive perturbation decreased the velocity of the system and did not require an immediate stabilization. However, the transients of this sudden change in the direction of motion needed to be attenuated, which required that the system enter a contraction

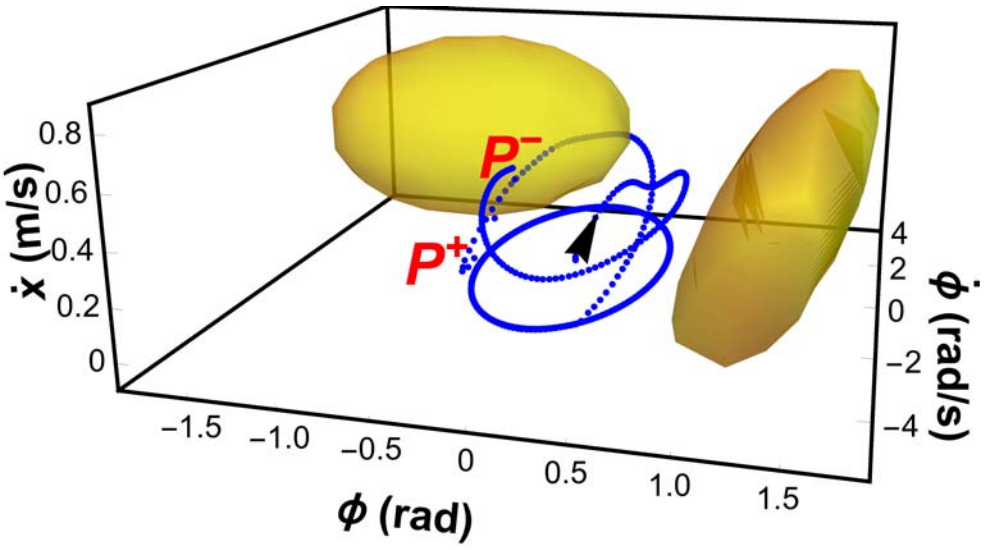

Fig. 7. A late trial with resistive perturbations. The subject passed through the contraction region after the perturbation to stabilize the trajectory.

region after the perturbation.

VI. Conclusion and Future Work

This work examined a complex interactive task of transporting an underactuated dynamic object, a cup of coffee, to reveal human motor control strategies. We showed that humans exploited contraction regions of the unforced, free system to compensate for known perturbations. Future work will examine whether these human control principles can enhance dexterous manipulation capabilities of robots. We envisage that "contraction-based" control will naturally lead to robust manipulation, particularly in physically interactive tasks. Moreover, we would like to investigate the generality of this control strategy in human motor control, and whether it extends to other types of tasks.

References

[1] S. Schaal, "Dynamic movement primitives - a framework for motor control in humans and humanoid robotics," in *Adaptive motion of animals and machines*, 2006, pp. 261–280.

[2] M. Ciocarlie, C. Goldfeder, and P. Allen, "Dimensionality reduction for hand-independent dexterous robotic grasping," in *IEEE/RSJ International Conference on Intelligent Robots and Systems (IROS)*, 2007, pp. 3270–3275.

[3] M. T. Ciocarlie and P. K. Allen, "Hand posture subspaces for dexterous robotic grasping," *The International Journal of Robotics Research (IJRR)*, vol. 28, no. 7, pp. 851–867, 2009.

[4] C. Ott, B. Henze, G. Hettich, T. N. Seyde, M. A. Roa, V. Lippi, and T. Mergner, "Good posture, good balance: comparison of bioinspired and model-based approaches for posture control of humanoid robots," *IEEE Robotics & Automation Magazine*, vol. 23, no. 1, pp. 22–33, 2016.

[6] N. Sugimoto, V. Tangkaratt, T. Wensveen, T. Zhao, M. Sugiyama, and J. Morimoto, "Trial and error: Using previous experiences as simulation models in humanoid motor learning," *IEEE Robotics & Automation Magazine*, vol. 23, no. 1, pp. 96–105, 2016.

[5] C. Gehring, S. Coros, M. Hutler, C. D. Bellicoso, H. Heijnen, R. Diethelm, M. Bloesch, P. Fankhauser, J. Hwangbo, M. Hoepflinger *et al.*, "Practice makes perfect: An optimization-based approach to controlling agile motions for a quadruped robot," *IEEE Robotics & Automation Magazine*, vol. 23, no. 1, pp. 34–43, 2016.

[7] P. Maurice, M. E. Huber, N. Hogan, and D. Sternad, "Velocity-curvature patterns limit human–robot physical interaction," *IEEE Robotics and Automation Letters*, vol. 3, no. 1, pp. 249–256, 2018.

[8] R. Van der Linde and P. Lammertse, "Hapticmaster - a generic force controlled robot for human interaction," *Industrial Robot: An International Journal*, vol. 30, no. 6, pp. 515–524, 2003.

[9] N. Hogan, "Impedance control: An approach to manipulation," *Journal of Dynamic Systems, Measurement, and Control*, vol. 107, no. 1, 1985.

[10] M. Kawato, "Internal models for motor control and trajectory planning," *Current opinion in neurobiology*, vol. 9, no. 6, pp. 718–727, 1999.

[11] C. Takahashi, R. A. Scheidt, and D. Reinkensmeyer, "Impedance control and internal model formation when reaching in a randomly varying dynamical environment," *Journal of neurophysiology*, vol. 86, no. 2, pp. 1047–1051, 2001.

[12] J. R. Flanagan, E. Nakano, H. Imamizu, R. Osu, T. Yoshioka, and M. Kawato, "Composition and decomposition of internal models in motor learning under altered kinematic and dynamic environments," *Journal of Neuroscience*, vol. 19, no. 20, pp. RC34–RC34, 1999.

[13] J. R. Flanagan, P. Vetter, R. S. Johansson, and D. M. Wolpert, "Prediction precedes control in motor learning," *Current Biology*, vol. 13, no. 2, pp. 146–150, 2003.

[14] W. Lohmiller and J.-J. E. Slotine, "On contraction analysis for nonlinear systems," *Automatica*, vol. 34, no. 6, pp. 683–696, 1998.

[15] ——, "Contraction analysis of non-linear distributed systems," *International Journal of Control*, vol. 78, no. 9, pp. 678–688, 2005.

[16] E. M. Aylward, P. A. Parrilo, and J.-J. E. Slotine, "Stability and robustness analysis of nonlinear systems via contraction metrics and sos programming," *Automatica*, vol. 44, no. 8, pp. 2163–2170, 2008.